Canadian Science Publishing

ARTICLE

Evaluating methods for estimating mortality from acoustic telemetry data

Lisa K. Peterson, Michael L. Jones, Travis O. Brenden, Christopher S. Vandergoot, and Charles C. Krueger

Abstract: Mortality rates are major determinants of long-term sustainability of exploited fish populations, yet accurately estimating these rates can be challenging. We used simulations to evaluate nonspatial and spatial modeling approaches for estimating mortality rates from acoustic telemetry detection data. Data were generated assuming different receiver configurations (grids, lines), number of receivers, and mortality levels. Relative error rates for total mortality ranged from 0% to 83% for the nonspatial model and from 1% to 141% for the spatial model. Absolute error rates ranged from 0.00 to 0.11 for the nonspatial model and from 0.01 to 0.15 for the spatial model. Accuracy and precision in mortality estimates were sensitive to assumed mortality rates and receiver configurations; the high-density receiver grid resulted in the lowest error rates. Estimates were consistently positively biased. We recommend using grid receiver configurations for mortality rate estimation from acoustic telemetry studies. The potential for biased mortality estimation from acoustic telemetry detection data should be considered during study design, particularly for those species with behavior and ecology that may result in long periods without detection.

Résumé : Bien que les taux de mortalité soient d'importants déterminants de la pérennité à long terme des populations de poissons exploitées, l'estimation exacte de ces taux présente son lot de défis. Nous avons utilisé des simulations pour évaluer des approches de modélisation non spatiale et spatiale pour estimer les taux de mortalité à partir de données de détection par télémétrie acoustique. Les données ont été générées en présupposant différentes configurations de récepteurs (grilles, lignes), différents nombres de récepteurs et différents degrés de mortalité. Les erreurs relatives sur la mortalité totale vont de 0 % à 83 % pour le modèle non spatial et de 1 % à 141 % pour le modèle spatial. Les erreurs absolues vont de 0,00 à 0,11 pour le modèle non spatial et de 0,01 à 0,15 pour le modèle spatial. L'exactitude et la précision des estimations de la mortalité sont sensibles aux taux de mortalité et à la configuration de récepteurs présumés; la grille de forte densité de récepteurs donne les erreurs les plus faibles. Les estimations présentent uniformément un biais positif. Nous recommandons d'utiliser des configurations de récepteurs en grille pour l'estimation des taux de mortalité à partir d'études de télémétrie acoustique. Le potentiel de biais dans les estimations de la mortalité à partir de données de détection par télémétrie acoustique devrait être pris en considération durant la conception d'études, particulièrement pour les espèces dont le comportement et l'écologie pourraient se traduire par de longues périodes sans détection. [Traduit par la Rédaction]

Introduction

Mortality rate is a critical population dynamics parameter for sustainable management of exploited fish populations; despite its importance, accurately estimating mortality rates remains challenging. Tagging studies in which fish are collected, tagged with individually unique or batch tags, and released back into the system where they were captured and possibly recaptured again (perhaps several times) during future sampling events (i.e., tag–recapture studies) are among the most frequently used methods for estimating mortality rates of fish populations. Methods for estimating mortality rates from tag–recapture studies have grown in complexity, but most are extensions of two key formulations: Jolly–Seber (JS) (Jolly 1965; Seber 1965) and Cormack–Jolly–Seber (CJS) formulations (Cormack 1964; Jolly 1965; Seber 1965). With the JS formulation, parameters of interest include survival, capture probability, population abundance, and number of new individuals entering the population. The CJS formulation is a restricted version of a JS formulation and is focused only on estimating survival and capture probability. Hereafter, our discussion of tag–recapture formulations is restricted to the CJS formulation.

Tagging studies inherently yield spatial data. Individual fish are generally collected (i.e., from discrete or multiple locations), tagged, and released, after which fish disperse from the capture–tagging site. Mortality rates that tagged individuals experience also generally vary spatially because of differences in environmental conditions or where fishing activities are concentrated; consequently, overall survival of an individual depends on where that fish has been located. Also, sampling efforts to recapture tagged individuals can differ spatially. Both tag–recapture and tag–recovery (i.e., terminal recapture) frameworks for estimating mortality components have been expanded to account for the inherent spatial structure to tagging data (Royle et al. 2014; Vandergoot and Brenden 2014). In the case of tag–recapture studies, a spatial CJS framework has been proposed to include the locations of where recapture events occur and to address spatial aspects of recapture

Received 6 November 2020. Accepted 14 March 2021.

L.K. Peterson, M.L. Jones, and T.O. Brenden. Quantitative Fisheries Center, Department of Fisheries and Wildlife, Michigan State University, East Lansing, Michigan, USA.

C.S. Vandergoot and C.C. Krueger. Center for Systems Integration and Sustainability, Department of Fisheries and Wildlife, Michigan State University, East Lansing, Michigan, USA.

Corresponding author: Lisa K. Peterson (email: peter710@msu.edu).

data (e.g., movement patterns of tagged individuals; spatially and (or) temporally varying mortalities), while also allowing for sample site level covariates. In recent decades, spatial CJS models have been used in a variety of applications (Hightower et al. 2001; Borchers and Efford 2008; Royle et al. 2009; Gardner et al. 2010; Raabe et al. 2014; Cooke et al. 2016; Hightower and Harris 2017; López-Bao et al. 2018).

Electronic tagging technology such as acoustic telemetry can generate large datasets of repeated observations (i.e., recaptures via transmitter detections) of tagged fish with spatial coverage that is less dependent on where fishing or assessment surveys occur. As a consequence, detections from acoustically tagged fish hold a great deal of promise for estimating mortality rates of fish populations (Kraus et al. 2018; Villegas-Ríos et al. 2020). Acoustic telemetry involves implanting or attaching an electronic tag to a fish that periodically emits a uniquely identifiable signal that is then detected and recorded on receivers (i.e., listening stations) deployed across the study area in fixed positions for up to a year or more (passive monitoring). Acoustic telemetry research can also include active monitoring in which searches for tagged fish are conducted from mobile platforms, although in large systems such as oceans or the Laurentian Great Lakes, this approach may not be an efficient means for collecting detection data. Acoustic telemetry has been used to study behavior and movement of fish in rivers (Welch et al. 2009; Perry et al. 2010), small lakes (Hightower et al. 2001), large lakes (e.g., Laurentian Great Lakes; Hayden et al. 2014; Krueger et al. 2018), and oceans (Heupel et al. 2006; Hussey et al. 2015).

Our project sought to evaluate the accuracy of estimating total mortality rates of tagged fish from acoustic telemetry detection data using spatial and nonspatial models in a large freshwater or marine system. An individual-based model was used to simulate fish movements within a system resembling Lake Erie with movement behaviors based on observed movement patterns of walleye in the lake (Kershner et al. 1999; Wang et al. 2007; Hayden et al. 2018). Detection histories of tagged individuals were simulated assuming different receiver configurations (e.g., number of receivers, spatial placement of receiver stations) and different mortality rates of tagged fish. These detection histories were then used in spatial and nonspatial CJS models to evaluate the accuracy and precision of the two models in estimating mortality rates. Our aim was to evaluate performance of the different models when applied to data generated from an acoustic telemetry study and to provide guidance regarding receiver configurations to those interested in estimating mortalities of fish populations from acoustic telemetry studies.

Methods

Simulation framework

Acoustic telemetry detection data were simulated in R (R Core Team 2019) using functions from the glatos package (Holbrook et al. 2017). Four components were included in the simulation framework: (1) generation of movement paths; (2) generation of electronic transmitter (hereafter referred to as "tag") transmissions along those paths; (3) specification of receiver location; and (4) a distance function that defined the ability of the receiver to detect transmissions (i.e., detection probability). In addition, a mortality function removed fish from the simulation according to a specified mortality rate. These functions generated a spatially explicit time series of detections similar in form to actual telemetry data, with tag detection histories for each individual fish. The simulation framework described in this study reflects ongoing acoustic telemetry work for Lake Erie walleye, coordinated by the Great Lakes Acoustic Telemetry Observation System (GLATOS; Krueger et al. 2018) but is meant to represent a more general species – large lake situation and not directly match the dynamics of walleye or the configuration of receivers in Lake Erie.

Movement generation

Detection data for 200 fish were simulated within a space that resembled Lake Erie (Fig. 1); all fish were assumed to be released at the same time at one location in the western portion of the lake, which mimics past walleye tagging operations that have been conducted (Peat et al. 2015; Raby et al. 2018; Bade et al. 2019; Faust et al. 2019; Matley et al. 2020). Simulated fish were monitored over a period of three years. Modeled movement patterns were essentially a random walk, which is often used when modeling animal movement (Berg 1993; Turchin 1998; Humston et al. 2004). We based some of the parameters used in this simulation on the simulation framework used by Kraus et al. (2018), who evaluated different receiver grid scenarios based on the same walleye acoustic telemetry studies referenced above. Because movement characteristics of walleye in the wild were unknown, they evaluated a range of movement rates, 0.1 to 0.9 $m \cdot s^{-1}$, over a period ranging from 30 to 150 days. In our simulation, a movement rate of 0.05 $m \cdot s^{-1}$ was chosen in part due to the length of the simulation. Even at the lowest movement rate assumed by Kraus (0.1 $m \cdot s^{-1}$), movements of simulated fish could traverse the entire study system multiple times in a year, which we deemed unlikely for a system as large as that of the Great Lakes. At a movement rate of 0.05 $m \cdot s^{-1}$, the movement paths of the simulated fish more closely resembled a seasonal migratory pattern, with fish moving across the lake approximately two times during the year. This movement rate is much lower than the maximum speed measured for walleye evaluated by Peake et al. (2000) but was meant to reflect the net effect of active foraging and resting periods on movements of individual fish.

The other aspect of simulating fish movement was the turning angle. A new relative direction was randomly drawn every 100 m from a normal distribution with a mean of 0° and a standard deviation of either of 5° (100 fish) or 25° (100 fish). The two standard deviations were used to represent two groups of fish. The group with the smaller standard deviation ranged much further, as they had a greater chance of continuing to head in a similar direction to the previous time step. The group with the larger standard deviations tended to remain within a more confined area. This approach was used to reflect the idea of heterogeneity of fish movement within a population (Fig. 1). Evidence from past tagging studies suggests some walleye spend the whole year in the western and west-central basin of Lake Erie, while others (frequently old, large walleye) move from the western basin to the eastern basin and return during the year (Wang et al. 2007; Vandergoot and Brenden 2014; Raby et al. 2018). The components of fish movement, as well as all other values used to generate simulations, did not vary over time.

After release, remaining abundance of tagged fish was projected with an exponential population model where the true total mortality was one of the evaluated scenarios:

$$N_t = N_0 e^{-Zt}$$

Fish that died during the year were randomly selected; the precise time that an individual's death occurred was drawn from a uniform distribution encompassing the entire year. When a tagged fish died, it would stop moving and disappear from the study area in the simulation. Three different instantaneous mortality rate scenarios were used: 0.1, 0.4, and 0.6.

Transmission generation

Along each of the simulated movement paths, tag transmissions were generated using tag signal specifications. We assumed that each tag transmitted approximately every minute for a duration of 5 s. Although most field studies involving Lake Erie walleye routinely used delays with longer durations, for the purpose of this study, the 1-min delay was considered sufficient. In an

Fig. 1. (*a*) Movement path for a fish with a standard deviation (SD) = 5 for its turning angle. This fish would tend to be more far-ranging because it tends to continue moving in a similar direction. (*b*) Movement path for a fish with SD = 25 for its turning angle. This fish would tend to stay closer to where it was released because it tends to turn sharply, instead of continuing in a similar direction, which results in a more circular path. The red dot indicates the release location on Toussaint Reef. (Maps created in R (R Core Team 2019) using a CSV file of Lake Erie boundary coordinates, courtesy of Ann Marie Gorman.) [Colour online.]

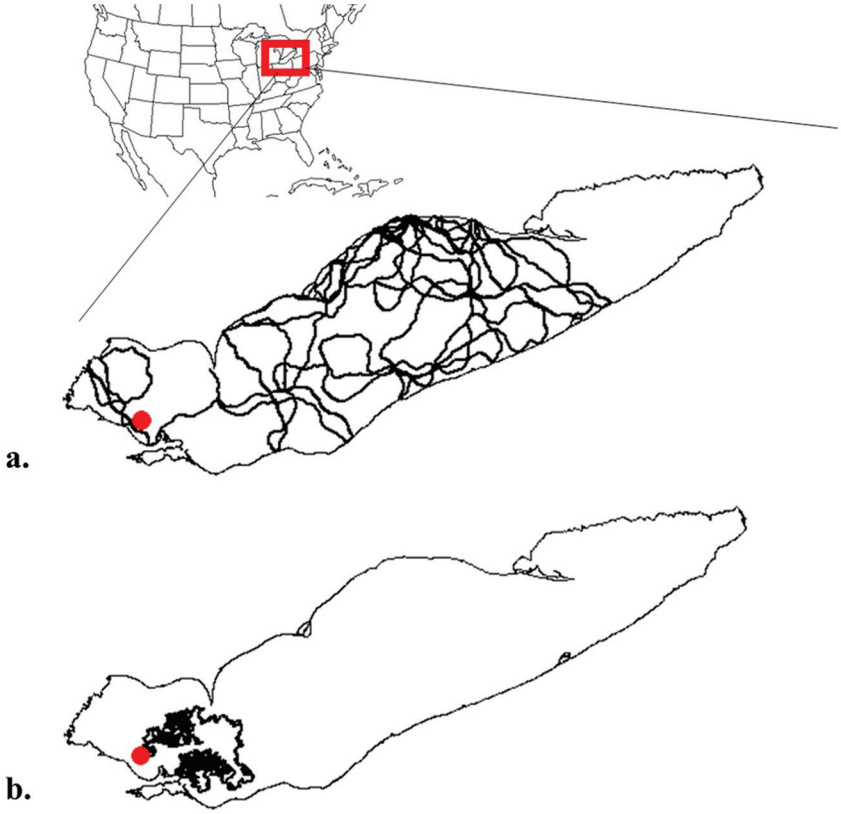

actual acoustic telemetry study, tag specifications are something that must be decided on by project investigators and require consideration about desired tag life and probability of tag detections to accomplish a project's objectives.

Receivers and detection generation

Whether a tag transmission was detected by a receiver depended on the assumed receiver configuration and the detection efficiency of the receivers. A detection probability function (or detection range curve) was used to represent the detection efficiency based on the distance between receivers and a tagged fish. In reality, the ability of a receiver to detect a tag transmission is highly dependent on environmental conditions (e.g., wind, waves, vegetation, ice cover, noise, and tag collisions; Kessel et al. 2014; Hayden et al. 2016), but it was beyond the scope of this research to incorporate those conditions into our simulation. The detection probability function that we used was an exponential decay function:

$$1 - \frac{1}{1 + 10^{-0.0025(D-800)}}$$

where D is the distance in metres between the receiver and the transmitting tag (Fig. 2). Under this equation, the probability of a receiver detecting the transmission of a tagged fish at a distance of 800 m was 50%. Alternatively, at distances of 400 or 1200 m, the probabilities of detection were approximately 91% and 9%, respectively. This represented "average" environmental conditions (Hayden et al. 2016; Kraus et al. 2018).

Different numbers (39 or 64 receivers) and spatial patterns (grids or lines) of receivers were used to evaluate how configuration affected model performance. Receiver lines have been used in the past to evaluate directional movement and to take advantage of choke points in rivers or lakes where a high confidence exists that fish will pass across the line at some point of the year. More recently, receiver grids have been used for more detailed information of fish movement (Kraus et al. 2018; Raby et al. 2018). For a 64-receiver grid configuration, receivers were spaced approximately 20 km apart, whereas a 39-receiver grid configuration resulted in a 25 km spacing. For the line configurations, receivers were distributed along four lines to represent lines across the basins of the study area (Fig. 3). Locations of lines did not differ based on the number of receivers being evaluated. Rather, the 64-receiver scenario just resulted in receivers being placed closer together in the line, which lessened the chance that a fish could cross the line without being detected.

The four receiver configurations combined with the three different mortality rate scenarios resulted in 12 total scenarios that were evaluated as part of this research. These 12 scenarios were replicated 10 times to evaluate the effect of the stochasticity in the simulation framework. The total amount of detections generated varied depending on the scenario, between 0.5 and 1.5 million total detections for 200 fish over three years.

Mortality estimation methods

Both the spatial and nonspatial models used to estimate total mortality were based on a CJS formulation (Cormack 1964; Jolly 1965; Seber 1965). As previously indicated, CJS frameworks use two parameters, survival rate (φ) and tag detection probability (p), to assign probabilities to each possible detection history (X_t). Survival rate represents the probability of an individual surviving from the previous time period to the current time period,

Fig. 2. Detection range function. Shape parameters of 0.0025 and 800. At 800 m, there is a 0.5 probability that the fish will be detected.

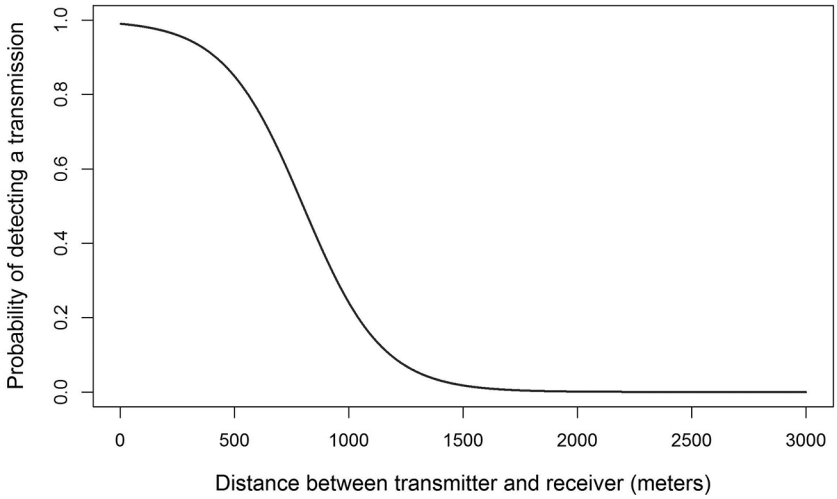

Fig. 3. Receiver configurations: (*a*) 64 (high-density) receivers in a grid; (*b*) 39 (low-density) receivers in a grid; (*c*) 64 (high-density) receivers set up in lines; and (*d*) 39 (low-density) receivers set up in lines. (Maps created in R (R Core Team 2019) using a CSV file of Lake Erie boundary coordinates, courtesy of Ann Marie Gorman.)

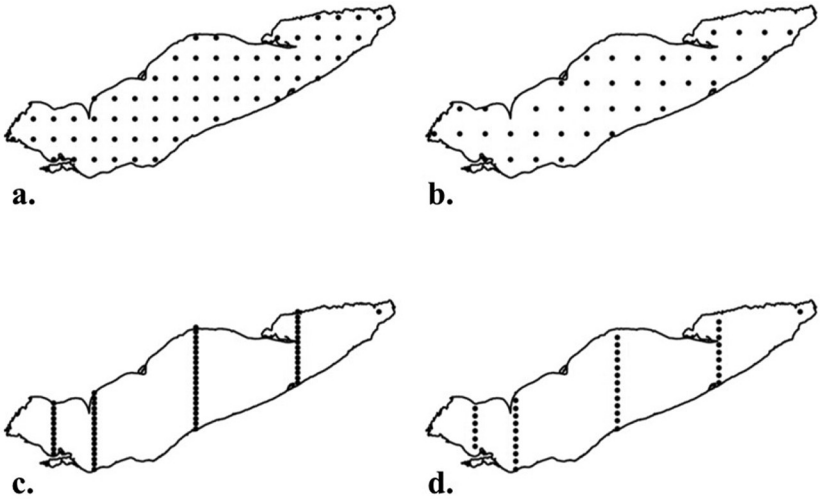

while detection probability is the probability of a surviving fish being detected in the current time period. Both models drew inferences from the simulated acoustic telemetry data, but the structure of the two models and processing of acoustic detections differed. Both models were estimated using Bayesian inference through JAGS (Plummer 2015) executed from within R (R Core Team 2019) via the jagsUI package (Kellner 2019).

Nonspatial model

For the nonspatial model, assuming N_0 represents the number of individuals released in a tagged cohort, the expected number of individuals $E(X_t)$ detected at time t can be expressed as

$$E(X_t) = N_0 \varphi_{t=1\rightarrow t} p_t$$

This basic structure was used for all possible detection histories. From Cormack (1964), a generalized form of the likelihood for the basic model would be

$$L \propto \prod_{t=1}^{n-1} (X_t)^{c_t} (\varphi_t)^{v_t} (p_{t+1})^{a_t+1} (1-p_{t+1})^{v_t-a_t+1}$$

with n indicating the total number of time periods, t indicating the current time period, c_t indicating the number of tagged individuals seen for the last time at time t, v_t indicating the number of marked animals known to be alive (detected at least once) after time t, and a_t indicating the number of individuals redetected in each sample. In the model used in this study, survival was assumed constant across time periods, while detection probability was allowed to vary through time; this allowed survival and detection probability to be estimated separately in the final time step. Detection probability was allowed to vary through time because all fish paths were started in the same location in the simulation; therefore, as time passed, the receivers further away from the release spot would have increasing detection probability due to fish dispersing throughout the lake. This model also ignored the specific moments within each time period that detections occurred, i.e., all detections in a month were aggregated together. Three parallel Markov chain Monte Carlo (MCMC) chains, each consisting of 10 000 iterations, were run from random initialization values with an initial 100-iteration adaptive phase. The first 1500 saved iterations were discarded as burn-ins and the chains were not thinned. Uniform prior distributions with lower

and upper bounds of 0 and 1, respectively, were assumed for survival and detection probabilities.

Spatial model

The spatial CJS model was implemented using a state–space framework. We based our approach on Gardner et al. (2010) and Raabe et al. (2014) spatial capture–recapture models. The state–space framework consisted of an observational model for the observed encounter histories of tagged fish, a state model for the "alive" state of the fish at each modeled time step, and a latent point process model that described the "activity centers" (i.e., estimated average locations) of tagged fish across the time periods. The observation model was conditional on the state model. The model was conditional on first recapture, so the initial detection was considered the first period for each individual and the state at that initial point was "alive". This means that if a fish was never detected after release, it was excluded from the analysis (this resulted in as many as 5% of the original 200 fish being excluded in any simulation run). Subsequent states were estimated using the probability of mortality from one time period to the next. The observation model for each receiver conditional on the state model of the individual was then assumed to be drawn from a distribution informed by the point process model.

The point process model, also called the latent activity center, described the average center of a fish's location during a sample period. This site was influenced by whether a fish was observed multiple times at a receiver as well as at what receivers it was detected during a single time step. The distance between a receiver and the estimated activity center influenced the tag detection probability for that receiver.

The formulation of this modeling approach incorporated counts of detections for each individual (i), at each receiver (j), during each sampling period (t, monthly). The observation model had encounter histories ($h(i, j, t)$) conditional on the state model ($z(i, t)$) with, as was mentioned earlier, the state in the initial time step assumed to be "alive", and all subsequent states modeled as

$$z(i, t) \sim \text{Bernoulli}[\varphi z(i, t-1)]$$

where φ was the survival probability from one time period to the next (monthly time step, $\varphi = e^{-Z/12}$). While this analysis assumed that survival was constant across space to allow a better comparison with the results of the nonspatial approach, this model could be extended to allow for spatially varying survival estimates.

This model allowed for multiple detections at any receiver during a time period. The data were count data and the observation model was conditional on the state model followed a Poisson distribution:

$$h(i, j, t)|z(i, t) \sim \text{Poisson}[\lambda_0 g(i, j, t) z(i, t)]$$

where λ_0 was the baseline detection rate, or the expected number of detections when an activity center and the receiver location were identical. The function $g(i, j, t)$ was a general distance function incorporating the distance between the individual activity center ($s(i, t)$) and the receiver location ($x(j)$). The distance function was a Gaussian kernel (or half-normal), a commonly used distance function used in sighting models:

$$g(i, j, t) = e^{-\frac{d(i,j,t)^2}{2\sigma^2}}$$

$$d(i, j, t) = s(i, t) - x(j)$$

where d was the Euclidean distance between an estimated individual activity center and the receiver, and σ was the scale parameter for the distance function. The distance function can be interpreted as the rate by which the detection probability of a specific receiver decreased as a function of distance from the estimated activity center. The location of the activity center was truncated by the specified state–space coordinates. The activity center locations were not constrained by the boundaries of the state–space itself, but by the upper and lower latitude and longitude values of the edges of the modeled system. As the modeled system was not a perfect rectangle, activity centers could be estimated in locations outside the bounds of the study system. More sophisticated modeling techniques would be needed to incorporate more complicated state–space shapes.

A random-walk approach was used for estimating activity center locations (Raabe et al. 2014) where activity center for an individual fish was informed by the location of the activity center in the previous time step. These activity centers were drawn from a normal distribution with a mean equal to the location of the activity center in the previous time step and a standard distribution, τ, which would correspond with the size of the movement of the individual between time intervals. Because we were dealing with activity centers in two dimensions, the random-walk process consisted of the following:

$$s_{x,i,t} \sim \text{Normal}(s_{x,i,t-1}, \tau_{x,i})$$

$$s_{y,i,t} \sim \text{Normal}(s_{y,i,t-1}, \tau_{y,i})$$

where the τ values were assumed to be drawn from a beta distribution. During time periods when fish were undetected, the model had trouble estimating activity center locations, similar to what was observed by Harris et al. (2021). Like Harris et al. (2021), we modified the random-walk process in an attempt to improve model convergence due to these nondetections. The modified random-walk process included the weighted average location of the fish in the time period that it was last detected (aa). In other words, when fish were not detected, the random-walk process consisted of the following:

$$\text{Fish not detected: } s_{x,i,t} \sim \text{Normal}(\text{aa}_{x,i,t \text{ of last detection}}, 50)$$

$$\text{Fish not detected: } s_{y,i,t} \sim \text{Normal}(\text{aa}_{y,i,t \text{ of last detection}}, 50)$$

The standard deviations for the random-walk process were not able to be estimated when fish were not detected; consequently, we assumed standard deviations of 50 in cases when fish were not detected.

The first activity center for each individual fish was estimated using uniform distributions with upper and lower limits equal to the boundaries of the study area. The model-assumed detections were instantaneous for each time period and ignored the specific time at which an individual was detected within the time period. Three parallel MCMC chains, each consisting of 15 000 iterations, were run from random initialization values with an initial 100-iterations adaptive phase. Bayesian inference analyzed these models, with three chains of at least 15 000 iterations. The first 2000 saved iterations were discarded as burn-ins. The chains were thinned; each tenth iteration was saved to calculate the final statistics. Uniform distributions were assumed as priors for φ (lower and upper boundaries of 0 and 1, respectively) and τ (lower and upper boundaries of 0 and 50, respectively). A gamma distribution with shape and rate parameters of 0.1 and 0.1, respectively, was assumed for p_0.

Convergence criteria

For both the nonspatial and spatial models, MCMC chain convergence for parameters was based on the potential scale reduction statistic ($\hat{R}$), which measures the stability of the Bayesian chains by taking the ratio of the average variance of the samples within each chain in the Bayesian analysis to the variance of pooled samples across all chains (Gelman et al. 2013). Ratios less than 1.1 were considered to indicate convergence. Trace plots of key parameters were also evaluated to ensure that burn-in (initial iterations that were discarded because of influence of starting

Fig. 4. Mortality estimates using the nonspatial model from the four scenarios (grid and line, 64 and 39 receivers) for 10 replicates. The point represents the estimate and the bars represent the 95% credible intervals. Circles are grids, triangles are lines, closed points are 39 receivers, and open points are 64 receivers. Each of the three panels represents a different true value of mortality: 0.1, 0.4, and 0.6.

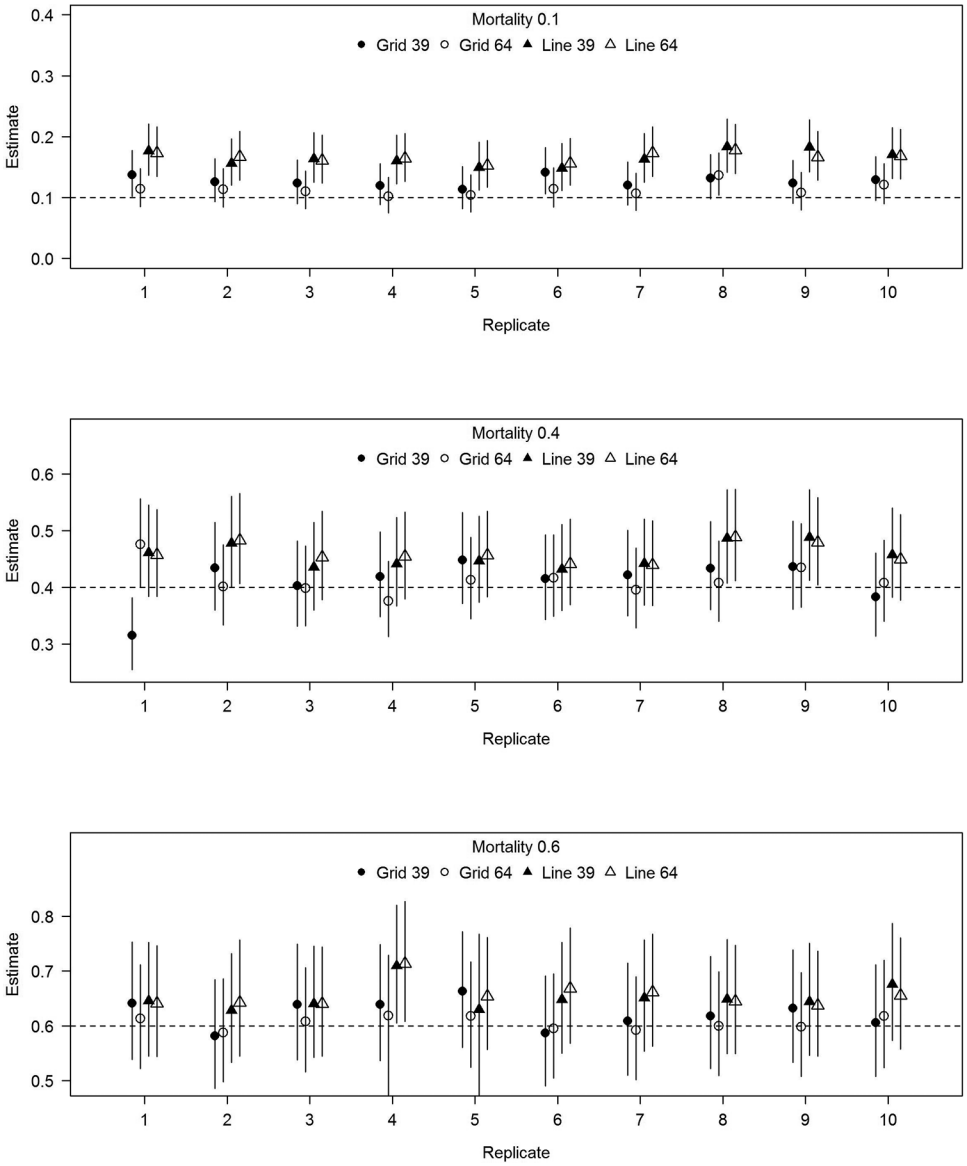

values) was sufficient and as another indicator of convergence (Brooks et al. 2011).

Results

Convergence

For the nonspatial model, all convergence criteria were met for all parameters in all scenarios. For the spatial model, the convergence criteria were met for all mortality estimates, but the model had difficulty estimating the activity centers. Across all scenarios, over 50% of the activity centers (out of a total of 7200 activity centers per scenario) met the convergence criteria. For many scenarios, 75% of activity centers met the convergence criteria. Even though the spatial model encountered difficulties in converging on stationary distributions for activity centers, we still proceeded with analyses of results given that we assumed that mortality was spatially invariant and thus the spatial location of a fish did not affect its probability of surviving. If mortality levels did vary spatially, the model's inability to estimate activity centers would likely prove more problematic.

Nonspatial model results

True mortality rate 0.1

The mortality estimates using the nonspatial model from the four scenarios and 10 replicates ranged from 0.10 to 0.18 (Fig. 4*a*). The relative error of the mortality estimates ranged from 2% to 83% (Fig. 5). The grid configuration consistently yielded more accurate estimates of mortality than the line configuration. The average mortality estimate for the grid configuration was 0.12, with the estimates ranging from 0.10 to 0.14; for the line configurations, the average mortality estimate was 0.17, with the estimates ranging from 0.15 to 0.18. Mortality estimates were more accurate with the higher number of receivers. For the 64-receiver grid configuration, the averaged mortality across all simulations was 0.11, with estimates ranging from 0.10 to 0.14. The 64-receiver grid configuration was the only configuration in which the 95%

Fig. 5. Relative error ((observed – true)/true) of mortality estimates (*M*) for all 120 scenarios using the nonspatial estimation approach.

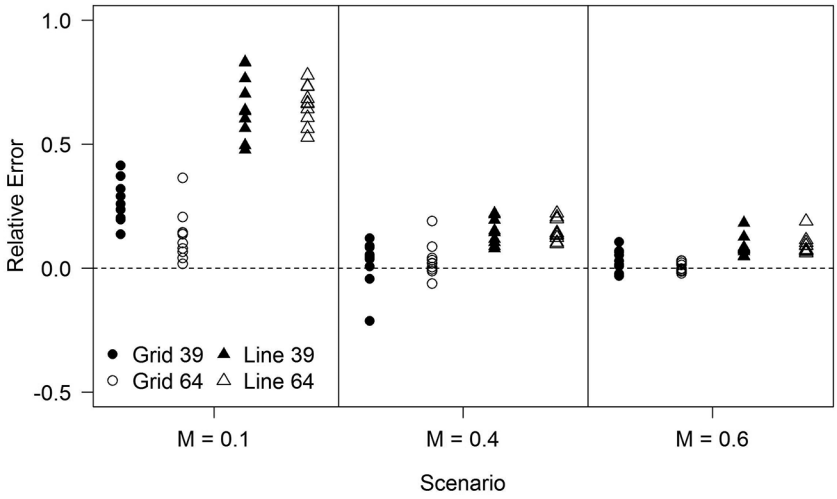

credible intervals for the mortality estimates encompassed the true mortality rate in all 10 replicates.

True mortality rate 0.4

The mortality estimates using the nonspatial model from the four scenarios and 10 replicates ranged from 0.31 to 0.49 (Fig. 4*b*). The relative error of the mortality estimates ranged from 0% to 22% (Fig. 5). The grid configuration consistently yielded more accurate estimates of mortality than the line configuration. The average mortality estimate for the grid configuration was 0.41, with estimates ranging from 0.31 to 0.48; for the line configuration, the average mortality estimate was 0.46, with the estimates ranging from 0.43 to 0.49. The average mortality estimate for both grid configurations was the same (0.41), with a range of 0.31 to 0.45 for the 39-receiver grid and 0.38 to 0.48 for the 64-receiver grid.

True mortality rate 0.6

The mortality estimates using the nonspatial model from the four scenarios and 10 replicates ranged from 0.58 to 0.71 (Fig. 4*c*). The relative error of the mortality estimates ranged from 0% to 19% (Fig. 5). The grid configuration consistently yielded more accurate estimates of mortality than the line configuration. The average mortality estimate for the grid configuration was 0.61, with the estimates ranging from 0.58 to 0.66, while for the line configuration, the average mortality estimate was 0.63, with the estimates ranging from 0.63 to 0.71. The 64-receiver grid configuration performed the best of the four scenarios, with an average mortality estimate of 0.60 and a relatively narrow range of estimates from 0.59 to 0.62. The relative error ranged from 0% to 3%.

Spatial model results

True mortality rate 0.1

The mortality estimates using the spatial model from the four scenarios and 10 replicates ranged from 0.13 to 0.24, showing a consistent positive bias (Fig. 6*a*). The relative error of the mortality estimates ranged from 31% to 141% (Fig. 7). The 64-receiver grid consistently outperformed the other configurations, with an average mortality estimate of 0.15 and estimates ranging from 0.13 to 0.17. In nine out of 10 replicates, estimates from the line configuration regardless of the number of receivers were closer to the true value of mortality than the 39-receiver grid; mortality estimates for the 39-receiver grid ranged from 0.20 to 0.24 and averaged 0.21. Conversely, the 39- and 64-receiver lines resulted in average mortalities of 0.19 (range: 0.16 to 0.21) and 0.18 (range: 0.17 to 0.20), respectively.

True mortality rate 0.4

The mortality estimates using the spatial model from the four scenarios and 10 replicates ranged from 0.41 to 0.53, showing a consistent positive bias (Fig. 6*b*). The relative error of the mortality estimates ranged from 1% to 32% (Fig. 7). The 64-receiver grid configuration consistently outperformed the other configurations, with an average mortality estimate of 0.44 and estimates ranging from 0.41 to 0.46. In seven out of 10 replicates, the line configuration estimates regardless of the number of receivers were closer to the true value of mortality than the 39-receiver grid configuration. Mortality estimates from the 39-receiver grid configuration ranged from 0.47 to 0.53 and averaged 0.50. Conversely, the mortality estimates from the 39-receiver line confirmation ranged from 0.45 to 0.51 and averaged 0.48, and the mortality estimates from the 64-receiver line confirmation ranged from 0.46 to 0.51 and averaged 0.48.

True mortality rate 0.6

The mortality estimates using the spatial model from the four scenarios and 10 replicates ranged from 0.62 to 0.75, showing a consistent positive bias (Fig. 6*c*). The relative error of the mortality estimates ranged from 4% to 25% (Fig. 7). The 64-receiver grid configuration consistently outperformed the other configurations, with an average mortality estimate of 0.64 and estimates ranging from 0.62 to 0.69. In six out of 10 replicates, estimates from the line configuration regardless of the number of receivers were closer to the true mortality rate than the 39-receiver grid configuration. Mortality estimates from the 39-receiver grid configuration ranged from 0.64 to 0.75 and averaged 0.70. For the 39- and 64-receiver line configurations, estimates ranged from 0.65 to 0.73 and 0.66 to 0.73 and averaged 0.68 and 0.67, respectively.

Comparison of nonspatial and spatial model results

The nonspatial model consistently outperformed the spatial model. Comparing the mortality estimates calculated using the spatial and nonspatial methods from the same simulated population of fish, the nonspatial mortality estimate was closer than the spatial estimate to the true mortality rate in 138 out of 140 scenarios. The average relative error for the nonspatial model was 20%, while for the spatial model, it was 38%. For mortality estimates from scenarios with a true mortality rate of 0.1, the average relative error for the nonspatial model was 43%, whereas for the spatial model, it was 84%. For a true mortality rate of 0.4, the average relative error for the nonspatial was 10%, while for the spatial model, it was 19%. For a true mortality

Fig. 6. Mortality estimates using the spatial model from the four scenarios (grid and line, 64 and 39 receivers) for 10 replicates. The point represents the estimate and the bars represent the 95% credible intervals. Circles are grids, triangles are lines, closed points are 39 receivers, and open points are 64 receivers. Each of the three panels represents a different true value of mortality: 0.1, 0.4, and 0.6.

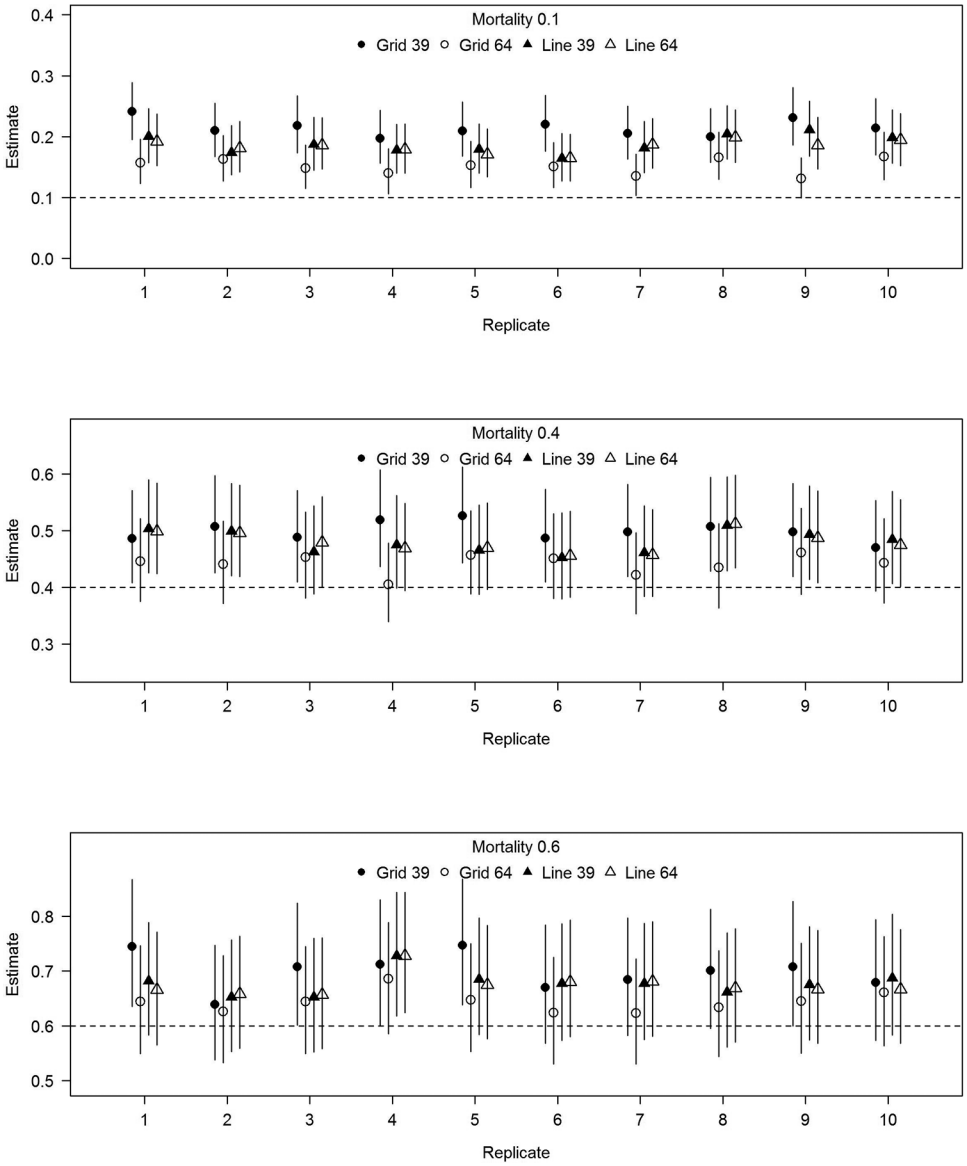

rate of 0.6, the average relative error for the nonspatial was 6%, while for the spatial model, it was 12%.

Discussion

The nonspatial model was more accurate and precise than the spatial model when estimating total mortality using acoustic telemetry data under the conditions assumed when simulating detection data. For both spatial and nonspatial models, grids with higher densities of receivers resulted in more accurate mortality rate estimates compared with line configurations; accuracy of both approaches improved with higher assumed mortality rates. Across all evaluated scenarios, mortality estimates for both modeling approaches were greater than the true, simulated values. The positive bias that we saw across scenarios likely resulted from confounding between receiver detection probabilities and fish death, both of which result in fish not being detected.

Our observation that a high-density grid configuration of receivers resulted in more accurate and precise estimates of mortality agrees with the results of other studies that have compared the configurations for estimating movement and habitat use (Kraus et al. 2018). Regardless of whether acoustic telemetry is used for characterizing mortality or movement, estimation accuracy depends on frequent detection of transmittered individuals and successfully identifying their fates (Villegas-Ríos et al. 2020). In large lentic systems, placing receivers in lines or gates in specific areas resulted in large areas of the system for which receiver coverage is poor or non-existent and may result in fish going long periods of time without being detected. This may lead models to identifying individuals as being dead when they are actually alive and actively swimming but in areas where no detections are possible. A similar situation may arise with grid configurations with a low number of receivers because the spacing among receivers is too large. Our finding that a high-density grid configuration resulted in more accurate estimates than a line configuration is analogous to observations from other mark–recapture study evaluations that found uniform sampling

Fig. 7. Relative error ((observed – true)/true) of mortality estimates (*M*) for all 120 scenarios using the spatial estimation approach.

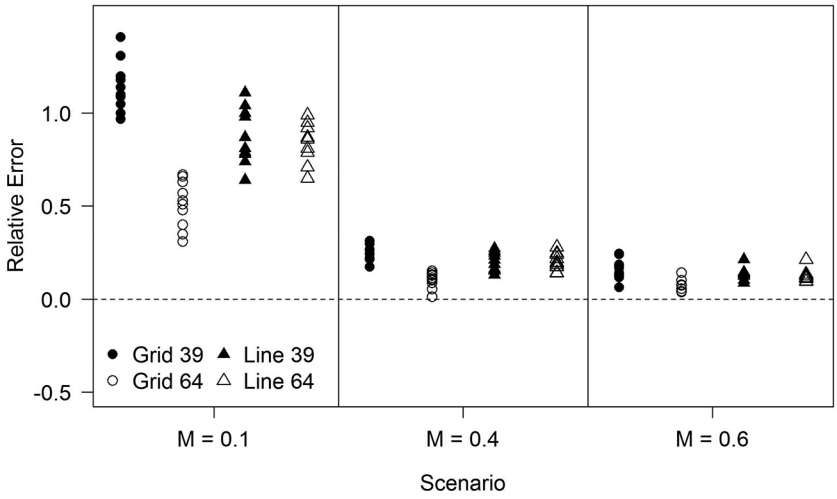

effort resulting in more accurate estimates than non-uniform sampling effort (Stevens 1997). This is not meant to suggest that deployment of lines or gates of receivers are never appropriate. Receivers configured in lines would be useful for telemetry studies where the main aim was to quantify coarse-scale movements such as whether fish cross management boundaries or the occurrence of interbasin or interlake emigration (e.g., Welch et al. 2009; Kessel et al. 2014). However, when the aim is mortality estimation, as in this study, high-density grids were the better study design.

The ability to accurately estimate fish survival from acoustic telemetry detection data will depend heavily on collecting enough detection data to be able to adequately characterize the fate of tagged individuals. Consequently, the exact configuration of receivers that should be used in a study should depend on the behavior and ecology of study organisms. In this study, we simulated detection data based on movement patterns of walleye in Lake Erie. Results could change for fish that show different movement behaviors. For more mobile species, fish may be more likely to encounter receivers, which may mean that fewer receivers need to be deployed and may reduce the bias associated with the estimation approach. Conversely, for more sedentary species, the required receiver coverage may become cost prohibitive, and an alternative evaluation technique should perhaps be considered: for example, active telemetry in which searches for fish are conducted from a mobile platform (Pepperell and Davis 1999; Hightower et al. 2001) or strategically placed receivers, e.g., placing receivers at the mouths of the rivers of migrating fish or on the spawning site of a species that has a high spawning site fidelity (Binder et al. 2016; Hayden et al. 2018). Alternatively, more complex state–space models such as those that take different "states" into account may yield better estimation performance (Stich et al. 2015; Hightower and Harris 2017).

The higher density receiver configurations outperforming the low-density configurations was an anticipated result — greater sampling effort should produce more accurate estimates. As stated previously, the optimal density of receivers will be linked to the movement of the fish population being studied. In addition to fish species being sedentary and influencing results, space use by fish could influence optimal configurations as well. For example, fish that remain close to shore may be missed by receivers in open water. High-density grids and thus a higher sampling effort, especially if it can be informed by knowledge of where fish tend to be, are likely particularly important for species that show more localized movement patterns.

The true mortality rate influenced the relative error of the mortality estimation methods. The highest relative errors for both the nonspatial and spatial models across receiver configurations were when the lowest true mortality was simulated (0.1), and in all cases, these errors were overestimates of mortality. It is worth pointing out that a total mortality rate of 0.1 is likely on the lower range of mortality rates for exploited fish populations (Then et al. 2015). Relative error also obscures the consistency of the positive bias among mortality levels. The absolute error rates for total mortality for both the nonspatial and spatial model were fairly consistent across mortality rates; however, the high-density grid still resulted in lower error rates than the other receiver configurations. Positive bias may arise because both mortality estimation methods have difficulty accounting for fish that remain undetected, violating the assumption that detection was independent among sampling events and fish. Evaluating a wider range of scenarios could test this hypothesis. If this explanation is true, performance could be improved by using a higher receiver density in grids (and possibly lines) to decrease the chance of live fish remaining undetected in the study area.

This work did not evaluate the effect that the number of tags in a system has on the performance of the estimation methods. Receivers and acoustic tags are two of the main resource investments in acoustic telemetry studies. The methods described here (simulations to compare receiver configurations) could easily be extended to do a cost–benefit analysis of the trade-off between tag numbers and receiver density. By simulating different combinations of tags and receivers, the optimum study design could be identified given availability of resources.

A caveat with the results is the diagnostics of the activity center estimates. A component of the spatial model was estimating the center of activity for each individual in the population during each time step. The spatial model had difficulties estimating the activity centers for time periods when fish were not detected. Correlating activity centers from one time step to the next and using the last known detected average location of the fish alleviated some of the convergence issues, but diagnostics showed that a fraction (less than 25%) of the activity center estimates were unstable. It is possible that greater computing power and more efficient estimation algorithms than were available for this study could improve the activity center estimates. However, the difficulty with the estimation of the activity centers may always be present if instances occur when fish are not being detected. While the issues arising from non-detection could be alleviated by using a larger time step to decrease the number of non-detection

instances or further restricting the assignment of activity centers, this approach would also start to diminish the amount of spatial data used in the spatial model or limit the ability to look at spatial and temporal patterns in parameters. This suggests that the spatial model may be most useful when a high number of detections exist, for example, in river systems or small lakes.

Another important caveat of this work is the major assumptions made in the simulation framework that may differ from observed acoustic telemetry studies. In our simulation framework, all fish were released in the same location all at once, the dynamics of the fish populations were not spatially or temporally varying, the detection ability of the receivers was assumed and constant, fish were constantly and consistently moving, and the tag transmission rate was more than the average transmission rate of tags commonly used. These assumptions could affect the detectability and the dynamics of the tagged individuals and thus affect the results. Future work could explore more complex simulated dynamics such as temporally and spatially varying detection and survival probability to evaluate the consequences these have on the performance of the estimation methods.

Even though the nonspatial method performed better than the spatial approach and some limitations to these models exist as described above, spatial models may be able to capture variations in demographics in ways not illustrated by this simulation study. Mortality was assumed to be constant across space in the spatial method because the focus of the study was to compare the estimates from nonspatial and spatial methods. However, the spatial method could be used to evaluate spatial survival estimates. Mortality rates have been shown to vary spatially, and studies incorporating that variability into stock assessments show the importance of spatial structure for certain fish stocks (Berger et al. 2012; Vandergoot and Brenden 2014; Langseth and Schueller 2017). Fish populations experience different mortality vulnerability as they move across a landscape, for example, due to spatially varying fishing effort. If mortality was spatially varying, a spatial model would be able to identify the dynamics that a nonspatial model would ignore. A potential middle-ground approach was used by Perry et al. (2010), who used a discrete-space multistate CJS model to estimate survival and migration of juvenile Chinook salmon, which used four potential migration routes to incorporate spatial data into their analyses. This approach could be useful particularly in river systems. The underlying simulation framework in this study did not incorporate spatial heterogeneity of population dynamics, so the additional benefits of spatial mark–recapture models may not be captured in these results.

In summary, acoustic telemetry data can be used in nonspatial and spatial models to reasonably estimate the mortality of a fish population, although some limitations occurred with regards to the performance of the spatial model. The nonspatial estimation approach outperformed the spatial estimation approach, in terms of both relative error and convergence of the model parameters. The spatial estimation approach did show promise as a mortality estimation method, and more work should be done investigating these techniques and how they perform under different acoustic telemetry study designs. When designing acoustic telemetry studies with the objective of obtaining estimates of mortality and when the study site is similarly large and the movement dynamics of the fish are unknown or considered to have low spawning site fidelity, high-density receiver grids should be used and positive bias of mortality estimates should be considered, whether using a spatial or nonspatial estimation approach, particularly if the population is expected to have a low mortality rate. The high-density receiver grid configuration consistently provided more accurate estimates of mortality and would be the recommended receiver design.

Acknowledgements

We are grateful to the two anonymous reviewers whose constructive and insightful comments improved the quality of the manuscript. The authors thank Elise Zipkin for her contributions during the initial model development and Chris Holbrook for his contributions to the simulation framework and for his helpful comments on the initial drafts of this manuscript. This work was funded by the Great Lakes Fishery Commission through the Fishery Research program (project 2014_BEN_44032) as well as by way of Great Lakes Restoration Initiative appropriations (GL-00E23010). This paper is Contribution 92 of the Great Lakes Acoustic Telemetry Observation System (GLATOS). This article is also Contribution 2021-11 of the MSU Quantitative Fisheries Center. The authors acknowledge the support of Michigan State University High Performance Computing Center and the Institute for Cyber-Enabled Research.

References

Bade, A.P., Binder, T.R., Faust, M.D., Vandergoot, C.S., Hartman, T.J., Kraus, R.T., et al. 2019. Sex-based differences in spawning behavior account for male-biased harvest in Lake Erie Walleye (*Sander vitreus*). Can. J. Fish. Aquat. Sci. **76**(11): 2003–2012. doi:10.1139/cjfas-2018-0339.

Berg, H.C. 1993. Random walks in biology. Princeton University Press, UK.

Berger, A.M., Jones, M.L., Zhao, Y., and Bence, J.R. 2012. Accounting for spatial population structure at scales relevant to life history improves stock assessment: The case for Lake Erie walleye *Sander vitreus*. Fish. Res. **115–116**: 44–59. doi:10.1016/j.fishres.2011.11.006.

Binder, T.R., Riley, S.C., Holbrook, C.M., Hansen, M.J., Bergstedt, R.A., Bronte, C.R., et al. 2016. Spawning site fidelity of wild and hatchery lake trout (*Salvelinus namaycush*) in northern Lake Huron. Can. J. Fish. Aquat. Sci. **73**(1): 18–34. doi:10.1139/cjfas-2015-0175.

Borchers, D.L., and Efford, M.G. 2008. Spatially explicit maximum likelihood methods for capture–recapture studies. Biometrics, **64**: 377–385. doi:10.1111/j.1541-0420.2007.00927.x. PMID:17970815.

Brooks, S., Gelman, A., Jones, G.L., and Meng, X.L. 2011. Handbook of Markov Chain Monte Carlo. Chapman & Hall/CRC Press, London.

Cooke, S.J., Martins, E.G., Struthers, D.P., Gutowsky, L.F.G., Power, M., Doka, S.E., et al. 2016. A moving target — incorporating knowledge of the spatial ecology of fish into the assessment and management of freshwater fish populations. Environ. Monit. Assess. **188**: 239. doi:10.1007/s10661-016-5228-0.

Cormack, R.M. 1964. Estimates of survival from the sightings of marked animals. Biometrika, **51**: 429–438. doi:10.2307/2334149.

Faust, M.D., Vandergoot, C.S., Brenden, T.O., Kraus, R.T., Hartman, T., and Krueger, C.C. 2019. Acoustic telemetry as a potential tool for mixed-stock analysis of fishery harvest: a feasibility study using Lake Erie walleye. Can. J. Fish. Aquat. Sci. **76**(6): 1019–1030. doi:10.1139/cjfas-2017-0522.

Gardner, B., Reppucci, J., Lucherini, M., and Royle, J.A. 2010. Spatially explicit inference for open populations: estimating demographic parameters from camera-trap studies. Ecology, **91**(11): 3376–3383. doi:10.1890/09-0804.1. PMID: 21141198.

Gelman, A., Carlin, J.B., Stern, H.S., Dunson, D.B., Vehtari, A., and Rubin, D.B. 2013. Bayesian data analysis. Chapman & Hall/CRC Press, London.

Harris, C., Brenden, T.O., Vandergoot, C.S., Faust, M.D., Herbst, S.J., and Krueger, C.C. 2021. Tributary use and large-scale movements of grass carp in Lake Erie. J. Gt. Lakes Res. **47**(1): 48–58. doi:10.1016/j.jglr.2019.12.006.

Hayden, T.A., Holbrook, C.M., Fielder, D.G., Vandergoot, C.S., Bergstedt, R.A., Dettmers, J.M., et al. 2014. Acoustic telemetry reveals large-scale migration patterns of walleye in Lake Huron. PLoS ONE, **9**(12): e114833. doi:10.1371/journal.pone.0114833. PMID:25506913.

Hayden, T.A., Holbrook, C.M., Binder, T.R., Dettmers, J., Cooke, S.J., Vandergoot, C.S., and Krueger, C.C. 2016. Probability of acoustic transmitter detections by receiver lines in Lake Huron: results of multi-year field tests and simulations. Anim. Biotelem. **4**: 19. doi:10.1186/s40317-016-0112-9.

Hayden, T.A., Binder, T.R., Holbrook, C.M., Vandergoot, C.S., Fielder, D.G., Cooke, S.J., et al. 2018. Spawning site fidelity and apparent annual survival of walleye (*Sander vitreus*) differ between a Lake Huron and Lake Erie tributary. Ecol. Freshw. Fish, **27**: 339–349. doi:10.1111/eff.12350.

Heupel, M.R., Simpfendorfer, C.A., Collins, A.B., and Tyminski, J.P. 2006. Residency and movement patterns of bonnethead sharks, *Sphyrna tiburo*, in a large Florida estuary. Environ. Biol. Fishes, **76**: 47–67. doi:10.1007/s10641-006-9007-6.

Hightower, J.E., and Harris, J.E. 2017. Estimating fish mortality rates using telemetry and multistate models. Fisheries, **42**(4): 210–219. doi:10.1080/03632415.2017.1276347.

Hightower, J.E., Jackson, J.R., and Pollock, K.H. 2001. Use of telemetry methods to estimate natural and fishing mortality of striped bass in Lake Gaston, North Carolina. Trans. Am. Fish. Soc. **130**: 557–567. doi:10.1577/1548-8659(2001)130<0557:UOTMTE>2.0.CO;2.

Holbrook, C., Hayden, T., and Binder, T. 2017. glatos: A package for the Great Lakes acoustic telemetry observation system. Available from https://gitlab.oceantrack.org/GreatLakes/glatos.git.

Humston, R., Olson, D.B., and Ault, J.S. 2004. Behavioral assumptions in models of fish movement and their influence on population dynamics. Trans. Am. Fish. Soc. **133**: 1304–1328. doi:10.1577/T03-040.1.

Hussey, N.E., Kessel, S.T., Aarestrup, K., Cooke, S.J., Cowley, P.D., Fisk, A.T., et al. 2015. Aquatic animal telemetry: A panoramic window into the underwater world. Science, **348**: 1255642. doi:10.1126/science.1255642. PMID:26068859.

Jolly, G.M. 1965. Explicit estimates from capture–recapture data with both death and immigration — stochastic model. Biometrika, **52**: 225–247. doi:10.2307/2333826. PMID:14341276.

Kellner, K., 2019. jagsUI: A wrapper around 'rjags' to streamline 'JAGS' analyses. Available from https://github.com/kenkellner/jagsUI.

Kershner, M.W., Schael, D.M., Knight, R.L., Stein, R.A., and Marschall, E.A. 1999. Modeling sources of variation for growth and predatory demand of Lake Erie Walleye (*Stizostedion vitreum*), 1986–1995. Can. J. Fish. Aquat. Sci. **56**(4): 527–538. doi:10.1139/f98-193.

Kessel, S.T., Cooke, S.J., Heupel, M.R., Hussey, N.E., Simpfendorfer, C.A., Vagle, S., and Fisk, A.T. 2014. A review of detection range testing in aquatic passive acoustic telemetry studies. Rev. Fish Biol. Fish. **24**: 199–218. doi:10.1007/s11160-013-9328-4.

Kraus, R.T., Holbrook, C.M., Vandergoot, C.S., Stewart, T.R., Faust, M.D., Watkinson, D.A., et al. 2018. Evaluation of acoustic telemetry grids for determining aquatic animal movement and survival. Methods Ecol. Evol. **9**: 1489–1502. doi:10.1111/2041-210X.12996.

Krueger, C.C., Holbrook, C.M., Binder, T.R., Vandergoot, C.S., Hayden, T.A., Hondorp, D.W., et al. 2018. Acoustic telemetry observation systems: challenges encountered and overcome in the Laurentian Great Lakes. Can. J. Fish. Aquat. Sci. **75**(10): 1755–1763. doi:10.1139/cjfas-2017-0406.

Langseth, B.J., and Schueller, A.M. 2017. Calculation of population-level fishing mortality for single- versus multi-area models: application to models with spatial structure. Can. J. Fish. Aquat. Sci. **74**(11): 1821–1831. doi:10.1139/cjfas-2016-0295.

López-Bao, J.V., Godinho, R., Pacheco, C., Lema, F.J., Garcia, E., Llaneza, L., et al. 2018. Toward reliable population estimates of wolves by combining spatial capture–recapture models and non-invasive DNA monitoring. Sci. Rep. **8**: 2177. doi:10.1038/s41598-018-20675-9. PMID:29391588.

Matley, J.K., Faust, M.D., Raby, G.D., Zhao, Y., Robinson, J., MacDougall, T., et al. 2020. Habitat use conflicts with harvest quota allocation strategies for an apex predator in a large freshwater system. J. Gt. Lakes Res. **46**: 609–621. doi:10.1016/j.jglr.2020.03.014.

Peake, S., McKinley, R.S., and Scruton, D.A. 2000. Swimming performance of walleye (*Stizostedion vitreum*). Can. J. Zool. **78**(9): 1686–1690. doi:10.1139/cjz-78-9-1686, doi:10.1139/z00-097.

Peat, T.B., Hayden, T.A., Gutowsky, L.F.G., Vandergoot, C.S., Fielder, D.G., Madenjian, C.P., et al. 2015. Seasonal thermal ecology of adult Walleye (*Sander vitreus*) in Lake Huron and Lake Erie. J. Therm. Biol. **53**: 98–106. doi:10.1016/j.jtherbio.2015.08.009. PMID:26590461.

Pepperell, J.G., and Davis, T.L.O. 1999. Post-release behaviour of black marlin, *Makaira indica*, caught off the Great Barrier Reef with sportfishing gear. Mar. Biol. **135**: 369–380. doi:10.1007/s002270050636.

Perry, R.W., Skalski, J.R., Brandes, P.L., Sandstrom, P.T., Klimley, A.P., Ammann, A., and MacFarlane, B. 2010. Estimating survival and migration route probabilities of juvenile Chinook salmon in the Sacramento–San Joaquin River Delta. N. Am. J. Fish. Manage. **30**(1): 142–156. doi:10.1577/M08-200.1.

Plummer, M. 2015. JAGS version 4.0.0 user manual. Available from https://sourceforge.net/projects/mcmc-jags/files/Manuals/.

Raabe, J.K., Gardner, B., and Hightower, J.E. 2014. A spatial capture–recapture model to estimate fish survival and location from linear continuous monitoring arrays. Can. J. Fish. Aquat. Sci. **71**(1): 120–130. doi:10.1139/cjfas-2013-0198.

Raby, G.D., Vandergoot, C.S., Hayden, T.A., Faust, M.D., Kraus, R.T., Dettmers, J.M., et al. 2018. Does behavioural thermoregulation underlie seasonal movements in Lake Erie walleye? Can. J. Fish. Aquat. Sci. **75**(3): 488–496. doi:10.1139/cjfas-2017-0145.

R Core Team. 2019. R: a language and environment for statistical computing. R Foundation for Statistical Computing, Vienna, Austria. Available from https://www.R-project.org/.

Royle, J.A., Karanth, K.U., Gopalaswamy, A.M., and Kumar, N. 2009. Bayesian inference in camera trapping studies for a class of spatial capture–recapture models. Ecology, **90**: 3233–3244. doi:10.1890/08-1481.1. PMID:19967878.

Royle, J.A., Chandler, R.B. Sollmann, R., and Gardner, B. 2014. Spatial capture–recapture. Academic Press.

Seber, G.A.F. 1965. A note on the multiple-recapture census. Biometrika, **52**: 249–259. doi:10.2307/2333827. PMID:14341277.

Stevens, D.L. 1997. Variable density grid-based sampling designs for continuous spatial populations. Environmetrics, **8**: 167–195. doi:10.1002/(SICI)1099-095X(199705)8:3<167::AID-ENV239>3.0.CO;2-D.

Stich, D.S., Jiao, Y., and Murphy, B.R. 2015. Life, death, and resurrection: Accounting for state uncertainty in survival estimation from tagged grass carp. N. Am. J. Fish. Manage. **35**(2): 321–330. doi:10.1080/02755947.2014.996685.

Then, A.Y., Hoenig, J.M., Hall, N.G., and Hewitt, D.A. 2015. Evaluating the predictive performance of empirical estimators of natural mortality rate using information on over 200 fish species. ICES J. Mar. Sci. **72**(1): 82–92. doi:10.1093/icesjms/fsu136.

Turchin, P. 1998. Quantitative analysis of movement: Measuring and modeling population redistribution in animals and plants. Sinauer, Sunderland, Mass.

Vandergoot, C.S., and Brenden, T.O. 2014. Spatially varying population demographics and fishery characteristics of Lake Erie walleyes inferred from a long-term tag recovery study. Trans. Am. Fish. Soc. **143**: 188–204. doi:10.1080/00028487.2013.837095.

Villegas-Ríos, D., Freitas, C., Moland, E., Thorbjørnsen, S.H., and Olsen, E.M. 2020. Inferring individual fate from aquatic acoustic telemetry data. Methods Ecol. Evol. **11**(10): 1186–1198. doi:10.1111/2041-210X.13446.

Wang, H.-Y., Rutherford, E.S., Cook, H.A., Einhouse, D.W., Haas, R.C., Johnson, T.B., et al. 2007. Movement of walleyes in Lakes Erie and St. Clair inferred from tag return and fisheries data. Trans. Am. Fish. Soc. **136**: 539–551. doi:10.1577/T06-012.1.

Welch, D.W., Melnychuk, M.C., Rechisky, E.R., Porter, A.D., Jacobs, M.C., Ladouceur, A., et al. 2009. Freshwater and marine migration and survival of endangered Cultus Lake sockeye salmon (*Oncorhynchus nerka*) smolts using POST, a large-scale acoustic telemetry array. Can. J. Fish. Aquat. Sci. **66**(5): 736–750. doi:10.1139/F09-032.